

## ヘルムホルツ共鳴器列を取り付けたトンネル内を伝播する音響孤立波

阪大 基礎工 杉本信正 (Nobumasa SUGIMOTO)

### Abstract

It is demonstrated theoretically that an acoustic solitary wave can be propagated in a tunnel with a periodic array of Helmholtz resonators, if the dissipative effects are made negligibly small. As wave propagation in such a periodic system is known as the Bloch waves, the array can give rise to the dispersion necessary to formation of the solitary wave. Explicit profiles of the solitary waves are shown by solving the steady-wave solutions to the nonlinear wave equations derived previously. It is found that the solitary wave is *compressive* and that it is propagated with a speed slower than the usual sound speed  $a_0$ , i.e. *subsonic*, but faster than  $a_0(1 - \kappa/2)$  in the linear long-wave limit,  $\kappa$  being a small parameter representing the ratio of the cavity's volume to the tunnel's volume per axial spacing between the neighboring resonators. As the propagation speed approaches the upper bound, the height of the solitary wave increases to approach the limiting height, while as the speed approaches the lower bound, the solitary wave tends to be the soliton solution of the Korteweg-de Vries equation. It is also found that while no solutions exist for the speed below the lower bound, the shock wave may be propagated for the speed above the upper bound, i.e. *supersonic*, but accompanying nonlinearly oscillatory wavetrain downstream.

### 1. Introduction

It has long been believed that an acoustic soliton<sup>†</sup> cannot exist in the pure air. For the air itself is not a dispersive material but rather a dissipative one. Of course, the dispersion occurs geometrically but it is too strong to balance with the weak nonlinearity for the soliton to be generated.

But it was recently revealed theoretically that the soliton is possible even in the acoustic waves propagating in a tunnel, if a suitable array of Helmholtz resonators (called simply resonators hereafter) is connected as shown in Fig.1 [1]. This was discovered in the course of the investigations to inhibit emergence of the acoustic shock wave generated by travelling of a high-speed train in a tunnel [2]. In the further study, it was shown that for the acoustic soliton to be generated, the array of the resonators can be generalized to the periodic array of any side branches as far as they are closed and acoustically compact [3, 4].

Wave propagation in such a periodic system may be termed the acoustic Bloch waves [5, 6] by analogy with that in the quantum mechanics [7]. The spatial periodicity gives rise to the dispersion even in the mode of plane waves. For nonlinear acoustic Bloch waves, the Korteweg-de Vries (K-dV) equation can be derived commonly under the continuum

<sup>†</sup>By the soliton, we mean a solitary wave as the steady-wave solution to the Korteweg-de Vries equation.

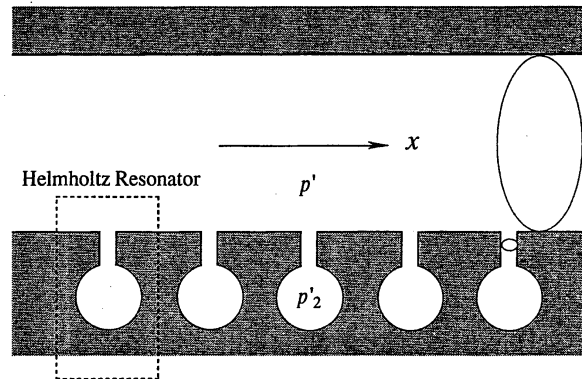


Figure 1. A tunnel with a periodic array of Helmholtz resonators.

approximation for distribution of the side branches [3,4]. This approximation holds substantially when a wavelength is much longer than the axial spacing between the neighboring side branches.

In view of these results, this paper abandons the assumption for the K-dV equation to be derived and investigates under what conditions a *solitary wave* is possible in steady propagation of nonlinear acoustic waves in the tunnel with the array of resonators. By neglecting all dissipative effects, we examine steady-wave solutions to the nonlinear wave equations derived previously [1]. It is noted that these equations still exploit the continuum approximation. The conditions for the steady-wave solutions to exist are clarified and their explicit profiles are displayed.

## 2. Governing equations

At the outset, we present the governing equations derived for the one-dimensional propagation of nonlinear acoustic waves in the tunnel with the array of resonators. If the dissipative effects due to the wall friction and the diffusivity of sound are negligibly small, they are given in the dimensionless form as follows (see (2.28) and (2.29) in [1]<sup>‡</sup>):

$$\frac{\partial f}{\partial X} - f \frac{\partial f}{\partial \theta} = -K \frac{\partial g}{\partial \theta}, \quad (2.1)$$

$$\frac{\partial^2 g}{\partial \theta^2} + \Omega g = \Omega f, \quad (2.2)$$

with  $f = f(X, \theta)$  and  $g = g(X, \theta)$  where the definitions of the symbols are briefly described in the following (see also Fig.1).

Denoting the small order of nonlinearity by  $\varepsilon$  ( $\ll 1$ ),  $\varepsilon f$  and  $\varepsilon g$  ( $f \sim g \sim O(1)$ ) denote the excess pressure  $p'$  and  $p'_2$  over the atmospheric  $p_0$  in the tunnel and in the

<sup>‡</sup>Note that  $\kappa$  in (2.28) is misprinted and is to be corrected as  $K$ .

cavity of the resonator, respectively, normalized in reference to  $p_0$  as  $[(\gamma + 1)/2\gamma]p'/p_0$  and  $[(\gamma + 1)/2\gamma]p'_2/p_0$  where  $\gamma$  stands for the ratio of the specific heats and the factor  $(\gamma + 1)/2\gamma$  is introduced for convenience. Letting the dimensional coordinate along the tunnel be  $x$  and the time be  $t$ ,  $X$  and  $\theta$  denote, respectively, the far-field coordinate  $\varepsilon\omega x/a_0$  and the retarded time  $\omega(t - x/a_0)$  in a frame moving with the usual linear sound speed  $a_0$ , where  $\omega$  is a typical angular frequency. The parameters  $K$  and  $\Omega$  measure the ratio of the smallness of the resonator to the nonlinearity and the ratio of the resonator's natural angular frequency  $\omega_0$  to  $\omega$ , defined, respectively, as follows:

$$K = \frac{\kappa}{2\varepsilon} \quad \text{and} \quad \Omega = \left(\frac{\omega_0}{\omega}\right)^2, \quad (2.3)$$

where  $\kappa$  ( $\ll 1$ ) is the ratio of the cavity's volume relative to the tunnel's volume per axial spacing between the neighboring resonators. These parameters may be removed from (2.1) and (2.2) by the replacement

$$(f, g) \rightarrow (Kf, Kg) \quad \text{and} \quad (X, \theta) \rightarrow (X/K\sqrt{\Omega}, \theta/\sqrt{\Omega}). \quad (2.4)$$

In the following, therefore,  $K$  and  $\Omega$  are set equal to unity without loss of generality.

### 3. Propagation of solitary waves

In search of a solitary wave, we examine steady-wave solutions to (2.1) and (2.2), assuming  $f$  and  $g$  depend on  $X$  and  $\theta$  only through a combination  $\theta - sX$  ( $\equiv \zeta$ ),  $s$  being a constant. The inverse of  $s$  gives the propagation velocity in the  $(X, \theta)$  space. But we shall see to what  $s$  corresponds in the original  $(x, t)$  space. Taking account of the replacement (2.4) and the definition of  $\Omega$ ,  $\zeta$  is written as

$$\zeta = \omega_0[t - (1 + \varepsilon K s)x/a_0] = \omega_0\{t - x/[a_0(1 - \varepsilon K s)] + O(K\varepsilon)^2\}. \quad (3.1)$$

Hence we find that  $a_0(1 - \varepsilon K s)$  corresponds to the original propagation velocity. Because  $\varepsilon K s$  is small enough, the propagation is directed toward the positive  $x$  axis irrespective of the sign of  $s$ .

Rewriting (2.1) and (2.2) in terms of  $\zeta$ , it follows that

$$-s \frac{df}{d\zeta} - f \frac{df}{d\zeta} = -\frac{dg}{d\zeta}, \quad (3.2)$$

$$\frac{d^2g}{d\zeta^2} + g = f. \quad (3.3)$$

For the solitary wave, we assume the undisturbed state far ahead as  $x \rightarrow \infty$  with  $t$  fixed. Thus the boundary conditions are imposed as follows:

$$f \rightarrow 0 \quad \text{and} \quad g \rightarrow 0 \quad \text{as} \quad \zeta \rightarrow -\infty. \quad (3.4)$$

Using these conditions, (3.2) is immediately integrated to give the first integral:

$$g = \frac{1}{2}f^2 + sf. \quad (3.5)$$

Next multiplying (3.3) by  $dg/d\zeta$  and writing  $fdg/d\zeta$  as  $f(f+s)df/d\zeta$  by (3.5), (3.3) is integrated with respect to  $\zeta$  where  $dg/d\zeta$  is assumed to vanish as  $\zeta \rightarrow -\infty$ , as inferred by (3.4). Further eliminating  $g$  by virtue of (3.5), it then follows that

$$\left(\frac{df}{d\zeta}\right)^2 = \frac{f^2(f_+ - f)(f - f_-)}{4(f+s)^2}, \quad (3.6)$$

with

$$(f_+ - f)(f - f_-) = -f^2 - 4\left(s - \frac{2}{3}\right)f - 4s(s-1), \quad (3.7)$$

and

$$f_{\pm} = -2\left(s - \frac{2}{3}\right) \pm \sqrt{-\frac{4}{3}s + \frac{16}{9}}, \quad (3.8)$$

where the sign is vertically ordered. In passing, it can be confirmed by (3.6) that  $df/d\zeta \rightarrow 0$  as  $f \rightarrow 0$  so that  $dg/d\zeta \rightarrow 0$  as  $\zeta \rightarrow -\infty$ .

In (3.6), a real solution  $f$  exists only when the right-hand side is non-negative. For it to be bounded,  $f_{\pm}$  must be real so that  $s \leq 4/3$ . Then the solution is possible in the interval  $f_- \leq f \leq f_+$ . Figure 2 shows the graph of  $f_{\pm}$  as the functions of  $s$ . For  $1 < s < 4/3$  or  $s < 0$ ,  $f_{\pm}$  are both negative or both positive. If so, the point  $f = 0$  is not included in the interval  $f_- \leq f \leq f_+$  and there cannot exist continuous solutions satisfying the boundary conditions (3.4). Therefore such a case should be excluded. For  $0 < s < 1$ , two types of the solutions are possible in the intervals  $0 \leq f \leq f_+$  or  $f_- \leq f \leq 0$ , separately. In the latter interval, however,  $df/d\zeta$  diverges as  $f \rightarrow -s$  because  $f_-$  is always less than  $-s$  for  $0 < s < 1$  (see Fig.2). The divergence implies that the legitimacy of (2.1) and (2.2) is lost since the dissipative terms in the original equations, especially the second-order derivative with  $\beta$  remain no longer small in the vicinity of the divergent point. Therefore we discard the solution in the interval  $f_- \leq f \leq 0$ .

In the interval  $0 \leq f \leq f_+$ , (3.6) is immediately led to the quadrature:

$$\int_f^{f_+} \frac{2(f' + s)}{f' \sqrt{(f_+ - f')(f' - f_-)}} df' = \pm \zeta. \quad (3.9)$$

This integral is straightforwardly executed to yield

$$4 \tan^{-1} \sqrt{\frac{f_+ - f}{f - f_-}} - \frac{2s}{\sqrt{-f_+ f_-}} \log \left| \frac{[\sqrt{-f_-(f_+ - f)} - \sqrt{f_+(f - f_-)}]^2}{(f_+ - f_-)f} \right| = \pm \zeta, \quad (3.10)$$

where the integration constant is chosen so that  $f$  takes the maximum value  $f_+$  at  $\zeta = 0$ .

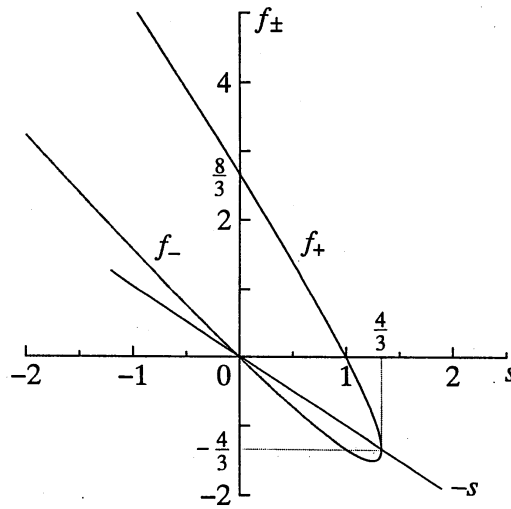


Figure 2. Graph of  $f_{\pm}$  versus  $s$ .

Figure 3(a) depicts the explicit profiles of  $f$  in  $\zeta$  for the values of  $s$  from 0.2 to 0.8 by the step 0.2, while Fig.3(b) depicts the profiles of  $g$  corresponding to those in Fig.3(a). As  $f$  tends to vanish, it is found from (3.10) that  $\zeta$  approaches both infinity so that  $f$  can also satisfy the undisturbed boundary conditions downstream as  $\zeta \rightarrow \infty$ . Hence the solution (3.10) represents the solitary wave symmetric with respect to  $\zeta = 0$ . As  $s$  becomes small, the height of the solitary wave  $f_+$  increases to approach the limiting value  $8/3$ . Exactly for  $s = 0$ , however, (3.10) ceases to be valid because  $f_-$  vanishes (while  $f_+ = 8/3$ ). Then  $f$  represents no longer the solitary wave but a sinusoidal wavetrain given by

$$f = \frac{8}{3} \cos^2 \left( \frac{\zeta}{4} \right). \quad (3.11)$$

This is also available by taking the limit of (3.10) as  $s \rightarrow 0$ . Then the first term on the left-hand side gives (3.11), whereas the second term drops out. It should be remarked that (3.11) cannot satisfy the boundary condition (3.4). Hence the height of the solitary waves is *less than*  $8/3$ .

As  $s$  approaches unity, on the other hand,  $f_+$  tends to vanish. In this limit, the propagation velocity in (3.1) approaches  $a_0(1 - \varepsilon K) = a_0(1 - \kappa/2)$ , which corresponds to the speed in the linear long-wave limit, though exactly given by  $a_0/(1 + \kappa)^{1/2}$  from the Bloch dispersion relation (see (64) in the reference [6]). Let  $s$  be  $1 - \alpha/3$  where  $\alpha$  ( $0 < \alpha \ll 1$ ) measures the closeness to unity. In terms of  $\alpha$ ,  $f_+$  and  $f_-$  are given, respectively, by  $\alpha + O(\alpha^2)$  and  $-4/3 + O(\alpha)$  to the lowest order. Then (3.10) is approximated to be

$$f = \alpha \operatorname{sech}^2 \sqrt{\frac{\alpha}{12}} \zeta, \quad (3.12)$$

with  $\zeta = \theta - X + \alpha X/3$ . This is nothing but the soliton solution to the K-dV equation [1]. Hence it is found that the soliton solution is included among the solitary-wave solutions in the limit as  $s \rightarrow 1$ .

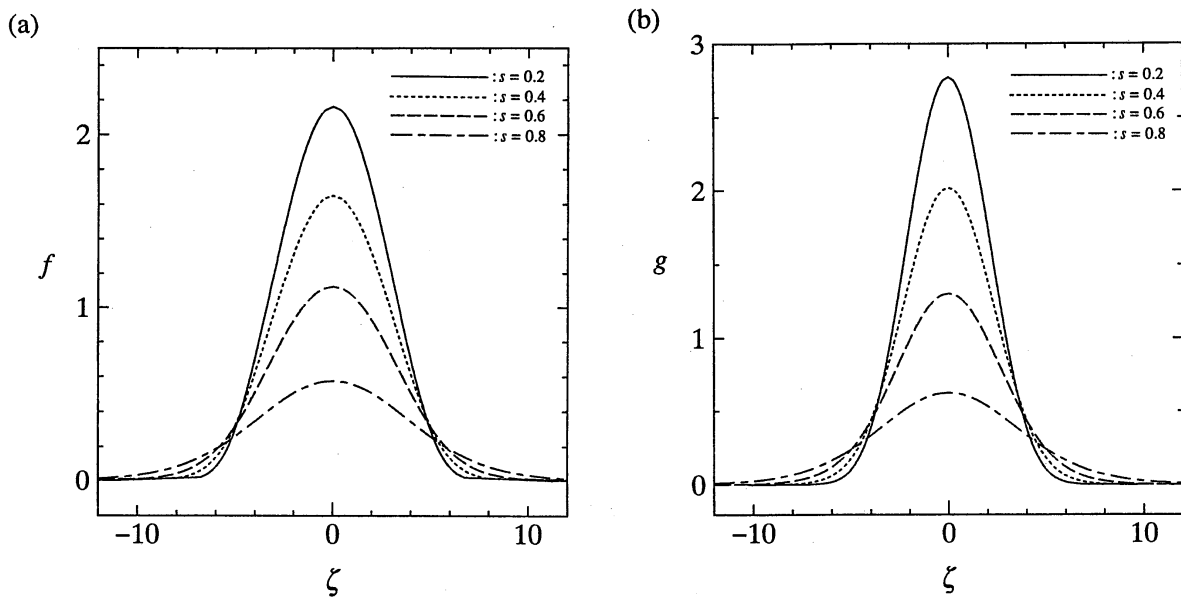


Figure 3. (a): Profiles of  $f$  for the solitary waves with  $K = 1$  where the solid, dotted, broken and chain lines represent, respectively, the profiles in the cases with  $s = 0.2, 0.4, 0.6$  and  $0.8$ . (b): Profiles of  $g$  calculated by (3.5) for the solitary waves corresponding to those of  $f$  in (a).

#### 4. Propagation of shock waves

So far, we have assumed  $0 < s < 1$ . Let us examine solutions for  $1 < s < 4/3$  or  $s < 0$ . Obviously, then, there cannot exist continuous solutions satisfying (3.4). But (3.2) and (3.3) allow a discontinuous solution as a weak solution. Let the discontinuity in  $f$  be located at  $\zeta = 0$ . In the vicinity of it, assume  $f$  be expressed approximately in the form  $f = f_1 h(\zeta)$  where  $h(\zeta)$  denotes the unit step function and  $f_1$  is an arbitrary constant representing the magnitude of discontinuity. Integration of (3.2) over a narrow region across  $\zeta = 0$  from  $\zeta = 0^-$  to  $\zeta = 0^+$  yields

$$\left[ sf + \frac{1}{2}f^2 - g \right]_{\zeta=0^-}^{\zeta=0^+} = 0, \quad (4.1)$$

where the square bracket  $[...]_{\zeta=0^-}^{\zeta=0^+}$  signifies a change of a quantity across  $\zeta = 0$ . In consistent with the step in  $f$ , (3.3) requires that

$$\left[ g \right]_{\zeta=0^-}^{\zeta=0^+} = \left[ \frac{dg}{d\zeta} \right]_{\zeta=0^-}^{\zeta=0^+} = 0. \quad (4.2)$$

While  $g$  and  $dg/d\zeta$  must be continuous across  $\zeta = 0$  due to the ‘inertia’ of the resonator, the magnitude of discontinuity  $f_1$  is found to be given by  $-2s$ . Although  $f_1$  may be arbitrary taken, it is known in the theory of gas dynamics that only the compressive shock wave ( $f_1 > 0$ ) is admissible. This prohibits taking a positive value of  $s$ . For  $s = 0$ , the discontinuity in  $f$  disappears but the higher-order derivative of  $f$  may be subjected to jump there. Therefore (3.11) can be adopted in the region  $\zeta > 0$  with a suitable shift

of the origin, while  $f$  is taken to vanish for  $\zeta < 0$ . Then the second-order derivative of  $f$  jumps across  $\zeta = 0$ .

Allowing the discontinuity at  $\zeta = 0$  in solutions, we now solve (3.2) and (3.3) for  $\zeta > 0$ . Of course,  $f$  and  $g$  are identically zero for  $\zeta < 0$ . The boundary conditions at  $\zeta = 0+$  are taken as follows:

$$f = f_1 = -2s \quad \text{and} \quad g = \frac{dg}{d\zeta} = 0 \quad \text{at} \quad \zeta = 0+ . \quad (4.3)$$

Integration of (3.2) leads to the same first integral as (3.5). Making use of this and (4.3), (3.3) is integrated, after multiplied by  $dg/d\zeta$ , to yield

$$\left(\frac{df}{d\zeta}\right)^2 = \frac{(f - f_1)}{4(f + s)^2} F(f; s) , \quad (4.4)$$

with

$$F(f; s) = -f^3 - \left(2s - \frac{8}{3}\right)f^2 - \frac{4}{3}sf + \frac{8}{3}s^2 . \quad (4.5)$$

In order to integrate (4.4), the roots of the cubic equation  $F(f; s) = 0$  must be specified. Examining the first-order derivative of  $F$  with respect to  $f$ , it is found that  $F$  has two extrema for  $s < 0$ , one in  $f < 0$  and the other in  $f > 0$ , and that both extremal values of  $F$  are positive. In fact, letting the extremum be located at  $f = f_e$ , we have

$$F(f_e; s) = -\frac{2}{3}\left(s - \frac{11}{9}\right)f_e^2 + \frac{8}{3}\left(s - \frac{f_e}{6}\right)^2 > 0 , \quad (4.6)$$

where  $f_e$  satisfies  $-3f_e^2 - 2(2s - 8/3)f_e - 4s/3 = 0$ . The above facts indicate that the cubic equation has one positive root  $f_2$  and two complex conjugate roots. Furthermore  $f_2$  is found to be greater than  $f_1$  and the limiting height  $8/3$  because

$$F(f_1; s) = 16s^2 > 0 , \quad F\left(\frac{8}{3}; s\right) = \frac{8}{3}s^2 - \frac{160}{9}s > 0 . \quad (4.7)$$

As  $-s$  increases,  $f_2$  also increases unlimitedly as well as  $f_1$  but the difference  $f_2 - f_1$  approaches the value 4. This is found from the asymptotic expression of  $f_2$  given by

$$f_2 = -2s + 4 + \frac{4}{s} + O(s^{-2}), \quad \text{as} \quad s \rightarrow -\infty . \quad (4.8)$$

Hence the solution to (4.4) with (4.5) is possible for  $f_1 \leq f \leq f_2$ . Equation (4.4) is then reduced to the integral:

$$\int_{f_1}^f \frac{2(f' + s)}{\sqrt{(f' - f_1)F(f'; s)}} df' = \pm \zeta . \quad (4.9)$$

The algebraic integrand can also be expressed in terms of the Jacobian elliptic function by introducing the following auxiliary variable  $z$  defined by (see the formulae 259.07 in [8], pp.134-135)

$$f' = \frac{c_1 f_2 (1 - \text{cn}z') + c_2 f_1 (1 + \text{cn}z')}{c_1 (1 - \text{cn}z') + c_2 (1 + \text{cn}z')} , \quad (4.10)$$

and

$$\text{cn}z = \frac{-c_2 (f - f_1) + c_1 (f_2 - f)}{c_2 (f - f_1) + c_1 (f_2 - f)} , \quad (4.11)$$

where  $\text{cn}z$  stands for the Jacobi's elliptic function  $\text{cn}(z, k)$  with the modulus  $k$  given by

$$k^2 = \frac{(f_1 - f_2)^2 - (c_1 - c_2)^2}{4c_1 c_2} , \quad (4.12)$$

and  $c_1$  and  $c_2$  are defined by

$$c_1^2 = H(f_1) = f_1^2 + c f_1 + \frac{8s^2}{3f_2} , \quad (4.13)$$

$$c_2^2 = H(f_2) = f_2^2 + c f_2 + \frac{8s^2}{3f_2} , \quad (4.14)$$

where  $H(f; s) = F(f; s)/(f_2 - f) = f^2 + c f + 8s^2/3f_2$  with  $c = f_2 + 2s - 8/3$ . It then follows from (4.9) that

$$\pm (\zeta - \zeta_0) = \frac{2}{\sqrt{c_1 c_2}} \int_z^{2K(k)} \left[ \frac{c_2 f_1 + c_1 f_2 + (c_2 f_1 - c_1 f_2) \text{cn}z'}{c_1 + c_2 - (c_1 - c_2) \text{cn}z'} + s \right] dz' . \quad (4.15)$$

where  $K(k)$  denotes the complete elliptic integral of the first kind, which should not be confused with  $K$  in (2.1) and  $\zeta_0$  is chosen so that  $f$  may take  $f_1$  at  $\zeta = 0$ .

This gives the form of the nonlinearly oscillatory wavetrain behind the shock wave. Upon integrating (4.15) numerically, Figure 4(a) depicts the profiles of  $f$  for the shock waves followed by the wavetrain where the solid and broken lines represent, respectively, the profiles in the cases with  $f_2 = 10$  ( $f_1 \approx 6.603$  and  $s \approx -3.301$ ) and  $f_2 = 5$  ( $f_1 \approx 1.968$  and  $s \approx -0.9839$ ), while the dotted line represents the sinusoidal wavetrain (3.11) for  $s = 0$ . Figure 4(b) depicts the profiles of  $g$  corresponding to those in Fig.4(a).

## 5. Results and discussions

Here we summarize the results of the analysis in the preceding sections. It is found that the steady propagation into the undisturbed state far ahead is classified, depending on the propagation velocity  $s$ , into two classes, one being the class of the solitary waves for  $0 < s < 1$  and the other that of the shock waves for  $s < 0$ . For  $s \geq 1$ , no steady-wave solutions can exist. The explicit profiles of  $f$  and  $g$  are obtained for  $K = \Omega = 1$ . For oth-

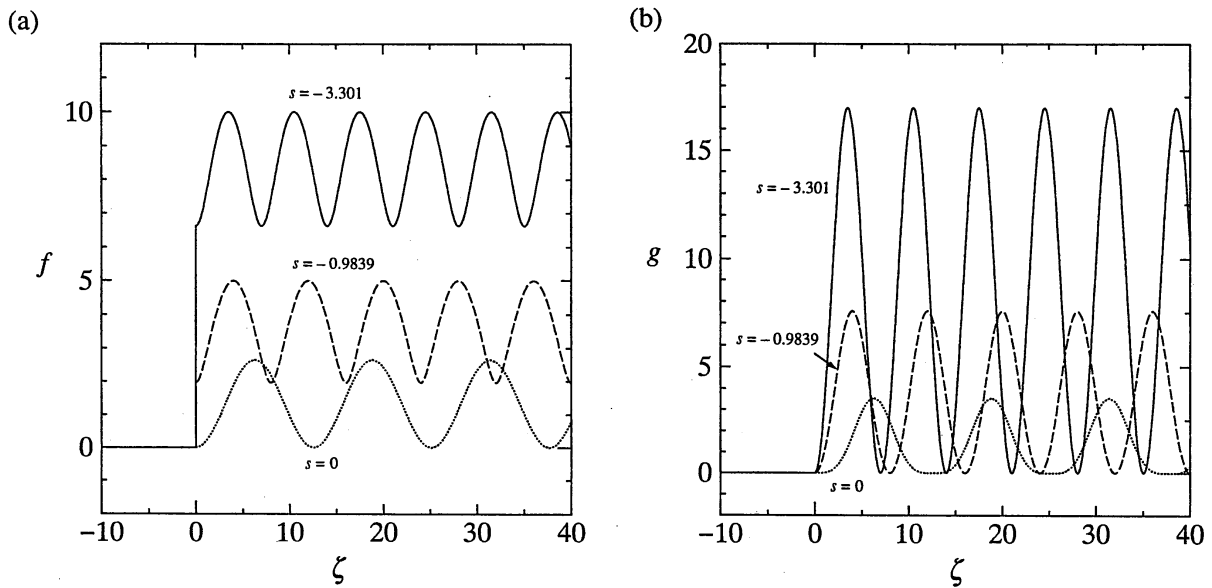


Figure 4. (a): Profiles of  $f$  for the shock waves with  $K = 1$  where the solid and broken lines represent, respectively, the profiles in the cases with  $f_2 = 10$  ( $f_1 \approx 6.603$  and  $s \approx -3.301$ ) and  $f_2 = 5$  ( $f_1 \approx 1.968$  and  $s \approx -0.9839$ ), while the dotted lines represent (3.11) for  $s = 0$ . (b): Profiles of  $g$  calculated by (3.5) for the shock waves corresponding to those of  $f$  in (a).

er values of  $K$ , the excess pressure  $\varepsilon f$  and  $\varepsilon g$  for the given profiles become large in proportion to  $K$ . On the other hand, the propagation velocity in the  $(x, t)$  space is retarded from the sound speed  $a_0$  by the amount  $\varepsilon K s$  proportional to  $K$  where note that  $\varepsilon K s$  is equivalent to  $\kappa s/2$  by the definition of  $K$  in (2.3). Hence while the shock waves are obviously *supersonic*, it is found that the solitary waves are *subsonic* but the speed is faster than  $a_0(1 - \kappa/2)$ .

As  $s$  decreases from unity, the height of the solitary wave increases monotonously (see Fig.3) while it is propagated faster. For  $s$  slightly below unity, the solitary wave is well approximated by the soliton solution of the K-dV equation. The deviation from unity determines the height of the soliton. As  $s$  tends to vanish from above, the height increases but it must be less than the limiting value  $8/3$  in the dimensionless form. This limiting height corresponds to the excess pressure  $p'_i$  given by

$$\frac{p'_i}{p_0} = \frac{8\gamma}{3(\gamma + 1)} \kappa. \quad (5.1)$$

As the solitary wave becomes higher, it is seen in Fig.3 that its width is reduced. One common check in identifying experimentally the solitary wave is to plot the half width against the maximum height. The half width  $\Delta$  is defined as  $2|\zeta(f_+/2)|$  when  $\zeta$  in (3.10) is regarded as the function of  $f$ . Figure 5 shows the relation between  $f_+$  and  $\Delta$  where the dotted line represents the relation between  $f_+$  and  $s$  given by (3.8). As  $f_+$  comes close to

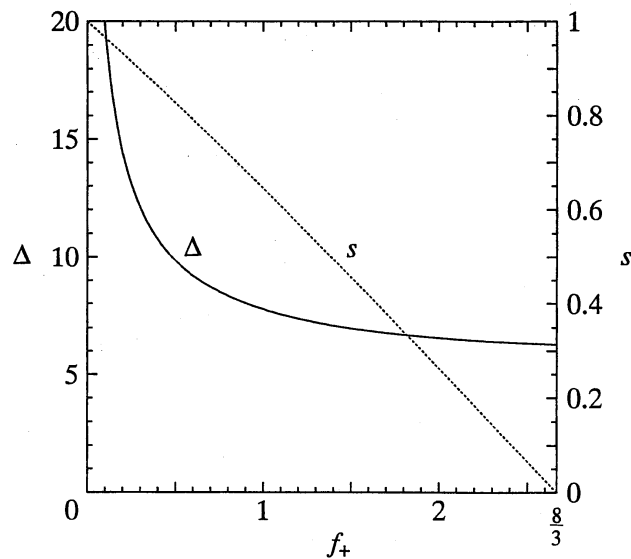


Figure 5. Relation between the maximum height of the solitary wave  $f_+$  and its half width  $\Delta$  where the dotted lines show the relation between  $f_+$  and  $s$  given by (3.8).

the limiting height  $8/3$ ,  $\Delta$  approaches  $2\pi$ , while as  $f_+$  tends to vanish,  $\Delta$  becomes inversely proportional to the square root of the height  $f_+ (= \alpha)$  (see (3.12)).

As was shown in [1], it is the case with  $\Omega \gg 1$  that the K-dV equation is derived asymptotically so that the soliton is possible. Let us see the connections between this approximation and the present results. Provided a typical frequency  $\omega$  for the solitary wave is defined as  $\pi/D$ ,  $D$  being a temporal half width in  $t$ , in other words,  $D$  is regarded as a half period of the sinusoidal wave of frequency  $\omega$ , then  $\Omega$  in (2.3) is given by  $(\omega_0 D/\pi)^2$ . Since  $\omega_0 D$  corresponds to  $\Delta$  in  $\zeta$ ,  $\Omega [= (\Delta/\pi)^2]$  is found to be greater than 4 for the limiting height. Hence it is found that the solitary wave exists for  $\Omega > 4$  in the present definition.

For a negative value of  $s$ , the shock wave appears with nonlinearly oscillatory wavetrain downstream and it propagates faster than the sound speed  $a_0$ . The greater the magnitude of discontinuity becomes, the faster it propagates. But the wavetrain tends to be a sinusoidal one with the peak-to-peak amplitude 4 and with period  $2\pi$  in  $\zeta$ . This is found by noting that as  $-s \rightarrow \infty$ , we have the relations that  $f_1 \approx f_2 \rightarrow -2s$ ,  $c_1 \approx c_2 \approx -2s$  and  $k^2 \rightarrow 0$  so that  $\pm(\zeta - \zeta_0)$  in (4.15) takes the value  $\pi - z$  with  $\cos \zeta_0 = -1$  and  $cnz$  is reduced to  $\cos \zeta$ . On the other hand, when the discontinuity vanishes for  $s = 0$ , the wavetrain is given by the sinusoidal one (3.11) with the peak-to-peak amplitude  $8/3$  and with period  $4\pi$  in  $\zeta$ . In terms of the frequency in  $t$ , the wavetrain for  $s = 0$  oscillates with the half of the resonator's natural frequency, while as  $-s \rightarrow \infty$ , it tends to oscillate with the natural frequency. For the intermediate values of  $s$ , it is observed in Fig.4 that the period becomes shorter as the shock wave becomes strong.

## 6. Conclusion

This paper has investigated the steady propagation of nonlinear acoustic waves in the tunnel with the array of Helmholtz resonators. It has been revealed that the compressive solitary wave is possible and its speed is subsonic but faster than  $a_0(1 - \kappa/2)$ , depending on the parameter  $\kappa$  for the smallness of the resonator. As mentioned in Introduction, the acoustic soliton is predicted universally in propagation along a long duct with a periodic array of side branches. But it should be noted that the solitary wave obtained here depends crucially on the specific type of the side branches, i.e. the response of the Helmholtz resonator in the present context. Therefore if other side branches are connected, solitary waves different in shape would be obtained.

Besides the solitary waves, it is found that the supersonic shock wave is also possible for the speed faster than  $a_0$ . But since the long-wave approximation breaks down at the shock front, it is evident that the validity of the solutions is lost in the exact sense. Yet it is worth emphasizing that the resonators are dormant in response to the discontinuous change in passage of the shock front and the long-wave approximation is still fully satisfied for the wavetrain. If we take account of a small effect due to the diffusivity of sound (represented by the second-order derivative with the small parameter  $\beta$  in the original equation (2.28)), the discontinuity is diffused to be replaced by a rapid but continuous transition layer.

## References

1. Sugimoto, N. 1992 Propagation of nonlinear acoustic waves in a tunnel with an array of Helmholtz resonators. *J. Fluid Mech.* **244**, pp.55-78.
2. Sugimoto, N. 1993 'Shock-free tunnel' for future high-speed trains. in *Proceedings of International conference on speed-up technology for railway and maglev vehicles*, (Japan Society of Mechanical Engineers, Tokyo) Vol.2, pp.284-292.
3. Sugimoto, N. 1993 On generation of acoustic soliton. In *Advances in Nonlinear Acoustics* (ed. H. Hobaek) pp.545-560. World Scientific.
4. Sugimoto, N. 1995 The generation of an acoustic soliton and soliton tube. *Proc. Estonian Academy of Sciences Physics & Mathematics* **44**, 1, pp.56-72.
5. Bradley, C. E. 1991 Acoustic Bloch wave propagation in a periodic waveguide. *Technical Report of Applied Research Laboratories, ARL-TR-91-19 (July)* (The University of Texas at Austin).
6. Sugimoto, N. & Horioka, T. 1995 Dispersion characteristics of sound waves in a tunnel with an array of Helmholtz resonators. *J. Acoust. Soc. Am.* **97**, pp.1446-1459.
7. Kittel, C. 1976 *Introduction to solid state physics*. (John Wiley & Sons, New York, 5th edition).
8. Byrd, P. F. & Friedman, M. D. 1971 *Handbook of Elliptic Integrals for Engineers and Scientists*. (Springer-Verlag, Berlin).